Proceedings of the XVII ECSMGE-2019
Geotechnical Engineering foundation of the future
ISBN 978-9935-9436-1-3

doi: 10.32075/17ECSMGE-2019-0696

XVII European Conference
ECSMGE 2019
Reykjavik
on Soil Mechanics
and Geotechnical Engineering

Screw pile design optimisation under tension in sand

Optimisation du dimensionnement sous tension des pieux vissés dans le sable

B. Cerfontaine
University of Dundee, Dundee, United-Kingdom

J.A. Knappett, M.J. Brown, C. Davidson, Y. Sharif
University of Dundee, Dundee, United-Kingdom

ABSTRACT: Many applications in offshore engineering, such as floating or jacket-founded wind turbines or wave energy converters, require a significant uplift capacity of their foundations to be kept in place. Straight-shafted or suction piles in sands have a limited uplift capacity as they resist by friction only. In contrast, screw piles or screw anchors are a promising solution which provides a similar capacity to plate anchors and does not generate disturbance for marine mammals (e.g. from pile driving operations). The optimisation of the screw pile design does not rely only on the geotechnical assessment of the uplift capacity based on soil strength, but also on operational (installation requirements) and structural (helix bending, core section stress, limiting steel plate thickness) constraints. This paper develops a methodology for the design optimisation of screw piles under pure tension in sand, incorporating all of these constraints, based on simplified analytical or semi-analytical approaches. The results show that the uplift capacity provided by an optimised screw pile is able to meet the needs of the offshore industry, across a range of soil densities and different applications (jacket foundation pile or tension leg platform anchor), providing that adequate installation plant could be developed to install them.

RÉSUMÉ: De nombreuses applications en géotechnique offshore, telles les éoliennes flottantes ou fondées sur des 'jackets', mais aussi les turbines houlomotrices, nécessitent des fondations possédant une capacité significative en tension. Les pieux classiques ou à succion on une capacité limitée en tension, car ils résistent uniquement grâce au frottement longitudinal. Les pieux ou ancrages vissés, au contraire, ont une capacité similaire aux ancrages plaques et ne génèrent pas de perturbation pour les animaux marins durant leur installation (contrairement aux pieux battus). L'optimisation des pieux vissés n'est pas basée uniquement sur la résistance du sol, mais également sur des contraintes géotechniques (durant l'installation) et structurales (flexion de l'hélice, résistance de la section centrale, épaisseur d'acier maximum). Cet article développe une méthodologie pour l'optimisation du dimensionnement des pieux vissés sous tension installés dans des matériaux sableux, sur base d'approches simplifiées analytiques ou semi-analytiques tenant compte des diverses contraintes. Les résultats montrent que la capacité optimale des pieux est suffisante pour plusieurs applications en géotechnique offshore ('jackets' out plateforme à tendons) et densités de sol, à condition qu'une machine de puissance suffisante puisse être développée pour assurer leur installation.

Keywords: Offshore Engineering; Screw anchors; uplift capacity

1 INTRODUCTION

Many applications in offshore geotechnical engineering require foundations/anchors with a significant tension capacity. Tension-leg platforms for the Oil & Gas industry (Randolph, 2011) or tension-leg floating wind turbines (Oguz, 2018) generate a maximum purely tensile loading onto their anchors (8-15MN). Wind turbines founded on tripod (Byrne, 2015) or jacket (Davidson, 2018b) structures, convert moment at the base of the turbine into a push/pull loading applied to the foundations (10-20MN). Wave energy converters inherently generate tension loading of several meganewtons (Gaudin, 2018). Finally, floating net-cage systems used in aquaculture also requires an engineered anchoring solution for offshore deployment (Huang, 2008), although of lower order of magnitude (0.15MN).

Screw piles are a promising anchoring solution, consisting of one or several helices attached to a core steel pile (Perko, 2009). Screw piles are literally screwed into the ground by applying a torque, generating less disturbance for marine mammals than conventional pile driving. The uplift capacity is mainly provided by the embedded helix which provides a larger long-term capacity than (suction) piles, which resist applied load only through shear mobilisation along the skirt and their own weight.

The maximum uplift capacity achievable for a given screw pile geometry is not only a function of the soil properties or embedment depth, but also of structural constraints (steel strength) or installation requirements for the installation device. The objective of this work is to derive a methodology enabling a rapid optimisation of screw pile design in sand and identification of the achievable performance envelope, considering installation and structural constraints.

2 METHODOLOGY

In the following, several simplified structural (core section requirements and helix bending) and geotechnical (uplift capacity, installation requirements) approaches are combined to calculate the maximum uplift capacity available for a given screw pile geometry embedded in sand.

2.1 Screw pile geometry

The screw pile geometry considered in the following is composed of a shaft and a single helix, as described in **Error! Reference source not found.**. The pile core is characterised by its length L, which corresponds to the embedment of the helix, its diameter D_c and wall thickness t_c. The helix is described by its diameter D_h and thickness t_h. Its pitch p_h is assumed constant and equal to $D_h/3$, which is in the range of many published studies ($0.15D_h$-$0.33D_h$) as summarised in (Cerfontaine, 2018). All of these dimensions, except the helix pitch, are considered as variables in the following analysis.

2.2 Installation Torque and force

The torque T required to install a screw pile at a depth L may be estimated from CPT results, based on the methodology presented in (Davidson, 2018a, 2018c). The torque is necessary to overcome the surface shear stresses acting on different parts of the screw pile and can be decomposed into different components (core/shaft

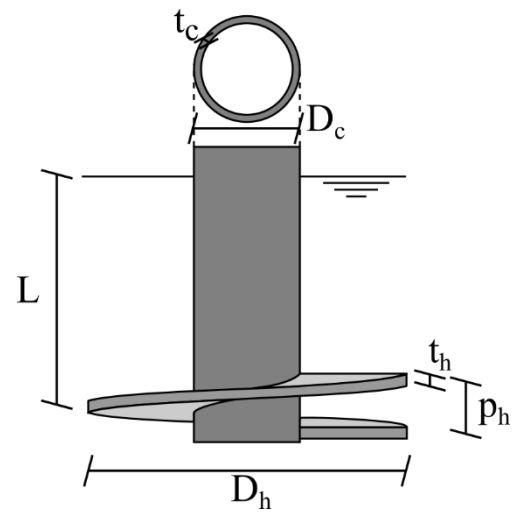

Figure 1 Geometry of the screw pile

T_c, base or tip T_b and helix T_h), all dependent on soil and geometrical properties such that

$$T(L) = \begin{array}{c} T_c(D_c^2, \bar{q}_c(L), \delta_{crit}, L) + \\ T_b(D_c^3, \bar{q}_c(L), \delta_{crit}) + \\ T_h\left(D_h^3, D_c^3, \bar{q}_c(L), \delta_{crit}, t_h, K_0\right) \end{array} \quad (1)$$

where $\bar{q}_c(L)$ is the averaged cone resistance q_c over $L \pm 1.5D_h$, δ_{crit} is the critical sand-steel friction angle and K_0 is the coefficient of lateral earth pressure at rest based on the sand critical state friction angle. The torque prediction also depends on a constant, the stress drop index a, used to calculate the lateral stress acting on the anchor and defined as $F_r/\tan\delta_{crit}$, where F_r is the CPT friction ratio.

The torque requirement increases non-linearly with the embedment depth, as represented in Figure 2 for a screw pile (D_h=1.7m, D_c=0.88m, t_h=100mm) embedded in dense sand. The required torque is dominated by the bottom (pile tip) component at shallow depth, while the core component becomes more prominent at larger depths. The maximum embedment depth that can be practically reached will depend on the maximum torque T_{max} that could be applied by the available installation device. For context, one of the largest current onshore installation devices,

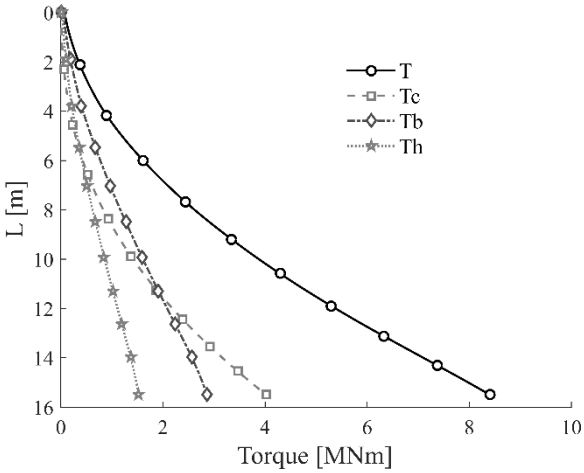

Figure 2 Torque requirement for a screw pile (Dc =0.88m, Dh=1.7m, th =100mm) embedded in dense sand (Dr = 82%)

the 'silent piler GRV2540' is able to install piles up to a diameter of 2.5m with a maximum torque equal to 3MNm (Giken, 2018).

A compression (or 'crowd') force must be applied at the top of the pile to ensure it penetrates the soil as a true helix movement to limit soil disturbance. Therefore a vertical displacement rate of one pitch, p_h per rotation must be achieved (Perko, 2009). The required force might be estimated as a function of soil and geometrical properties, similarly to the torque using , (Davidson, 2018c).

2.3 Core section requirement

The core section of the screw pile must be designed to sustain the combined torque and compression force applied during its installation. The maximum shear stress τ resulting from the torque T can be obtained from

$$\tau = 16\frac{T}{\pi}\frac{D_c}{D_c^4-(D_c-2t_c)^4}. \quad (2)$$

The compression force F generates a vertical stress σ_y within the section of

$$\sigma_y = \frac{4}{\pi}\frac{F}{\left(D_c^2-(D_c-2t_c)^2\right)}. \quad (3)$$

The Von Mises yield criterion is appropriate to account for the combined shear and normal stress in a steel tube, such that

$$\sqrt{\sigma_y^2 + 3\tau^2} \leq f_y \quad (4)$$

where f_y is the steel yield strength.

In addition, there is a limitation on the core wall thickness t_c, to ensure it is practically possible to manufacture it. It is assumed to be no larger than 10% of the core diameter D_c and lower than 100mm in any case.

2.4 Uplift capacity

The uplift capacity F_u of the screw pile is estimated through the semi-analytical approach proposed by Giampa *et al.* (2017) for plates. This approach assumes that a shallow failure mechanism develops within the soil. This mechanism has a

conical shape, emerges from the helix edge to the surface and its orientation to the vertical direction is equal to the peak dilatancy angle.

$$F_u = \left[1 + F_{s1}\frac{L}{D_h} + F_{s2}\left(\frac{L}{D_h}\right)^2\right]\gamma'\frac{\pi}{4}D_h^2 L \quad (5)$$

$$F_{s1} = 2F_{ps} \quad (6)$$

$$F_{s2} = \frac{4}{3}F_{ps}\tan\psi \quad (7)$$

$$F_{ps} = \tan\psi_p + \cos(\phi_p - \psi_p)\left(\tan\phi_p - \tan\psi_p\right) \quad (8)$$

where ϕ_p and ψ_p are the sand peak friction and dilatancy angles respectively and γ' is the buoyant sand unit weight. Al-Baghdadi (2018) found that the D_h/D_c ratio has an impact on the compression capacity, but is assumed it does not affect the uplift capacity.

This method was originally developed for L/D_h ratios lower than 5 (Giampa, 2017). Recent comparison with centrifuge test data has shown this criterion can be used up to L/D_h equal to 7.5, (Cerfontaine, 2018). However, the displacement required to fully mobilise the failure mechanism increases with depth. It is equal to $0.1D_h$ at L/D_h equal to 7.5, which is usually a practical limit used to define the ultimate tensile capacity.

Therefore, it has been decided herein to limit the maximum relative embedment ratio L/D_h to 8, in order to ensure Eq. (5) is still valid (shallow mechanism) and the displacement at failure remains limited to acceptable values.

2.5 Helix bending

The uplift load F_u applied at the top of the screw pile is balanced by the stress acting on the soil-soil interface along the failure mechanism. It is assumed that the load is transferred from the core to the soil through a uniformly distributed load q applied onto the helix, as represented in Figure 3, such that

$$q = \frac{4F_u}{\pi\left(D_h^2 - D_c^2\right)} \quad (9)$$

This uniform load generates bending within the helix, which is assumed to be represented

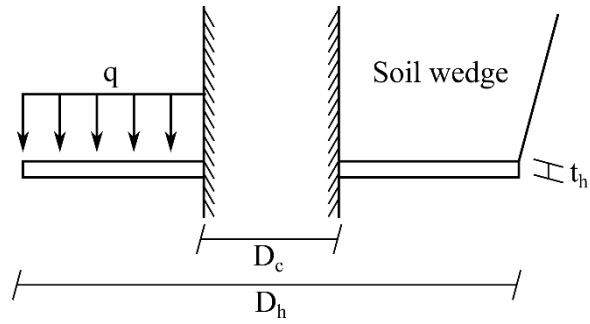

Figure 3 Idealisation of helix bending due to the load applied by the soil wedge

structurally as a horizontal plate connected to the shaft with full moment fixity. The maximum normal stress σ_x is induced at the helix-shaft connection and can be obtained as (Timoshenko, 1959)

$$\sigma_x = k\frac{qD_h^2}{4t_h^2} \le f_y \quad (10)$$

where k depends on the D_h/D_c ratio and is reported in Table 1. It is assumed the maximum stress allowable is equal to the steel yield strength f_y and the maximum helix thickness is limited to 100mm.

Table 1 Coefficient k, from (Timoshenko, 1959)

D_h/D_c [-]	1.25	1.5	2	3	4
k [-]	0.135	0.410	1.04	2.15	2.99

2.6 Analysis procedure

The optimisation problem is solved by varying systematically some of the parameters (D_h, D_c, T_{max}) and identifying for each of the combinations, the optimum uplift capacity F_u and embedment depths L that can be obtained, with respect to all constraints (core section capacity, helix bending, maximum plate thickness and relative embedment ratio). For a given set of geometrical parameters, the procedure is as follows.

1. Compute torque and force requirements for the given soil CPT data;
2. Calculate the maximum depth L_{max} constrained by: the maximum torque

applicable T_{max}, the section capacity (torque and compression) and the maximum relative embedment ratio L/D_h;
3. Compute the uplift capacity F_u and the minimum helix thickness t_h required to sustain bending;
4. If t_h is larger than the maximum plate thickness considered (100mm), reduce L_{max}.

3 RESULTS

3.1 Case studies

In this work, the screw pile design is optimised assuming it is embedded within a uniform layer of sand. Three contrasting soil conditions were investigated, considering the sand density to be loose (D_r = 38%), medium-dense (D_r = 52%) or dense (D_r = 82%). The peak strength properties (friction angle ϕ_p and dilatancy angle ψ_p), the critical state friction angle ϕ_{crit}, the soil-steel critical friction angle δ_{crit} and the buoyant unit weight γ' used are reported for each density in Table 2.

CPT tests were undertaken in-flight in the centrifuge at the University of Dundee (Davidson *et al.*, 2018). Results of the CPT cone resistance q_c are provided in Figure 4. The friction ratio F_r and CPT-soil friction angle, used to derive the stress drop index a as per (Davidson *et al.*, 2018), were 0.01 and 18° respectively. The steel yield limit f_y was assumed to be 350MPa.

Table 2 Properties of the three densities of HST95 sand, after (Al-Defae, 2013)

	D_r 38%	**D_r 52%**	**D_r 82%**
ϕ_p [°]	36.6	39.4	45.4
ϕ_{crit} [°]	32	32	32
ψ_p [°]	5.5	9	16.5
δ_{crit} [°]	24	24	24
γ' [kN/m³]	9.67	9.93	10.47

3.2 Maximum capacity for given geometry and installation torque

The uplift capacity of the screw pile is a non-linearly increasing function of L, as described in Eq. (5). The constraints limiting the maximum embedment are graphically shown in Figure 5, for an example geometry (D_h=1.5m, D_h/D_c=2, t_h = 0.1m, t_c = 0.075m) and a dense sand.

Figure 5(a) describes the evolution of the uplift capacity F_u and torque requirement T as the embedment L increases. Figure 5 (b) describes the evolution of equivalent stress induced within the core during screw pile installation σ_{eq} as well as the stress resulting from helix bending at σ_x.

The different constraints are also represented in these figures. The relative embedment ratio L/D_h has been limited to 8. The torque applicable is limited by machine capacity (5MNm in this case). The maximum stresses induced within the screw pile (σ_{eq} or σ_x) are limited to the yield stress f_y (350MPa). In this case, the maximum embedment is limited by the helix bending, as show in Figure 5 (b).

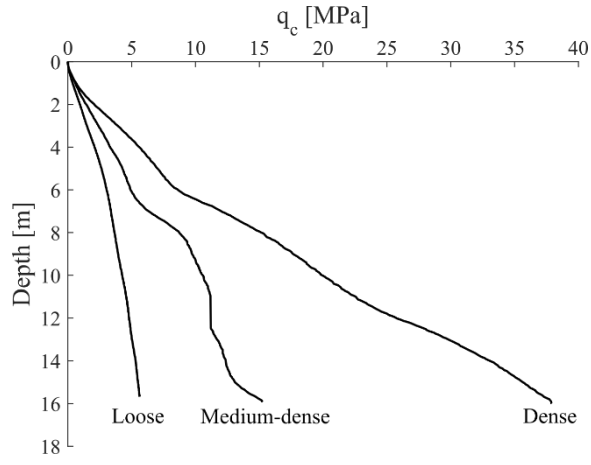

Figure 4 Results of centrifuge CPT tests at prototype scale (Davidson et al., 2018): cone resistance qc

3.3 Optimal design for a given torque

An example of the evolution of the maximum embedment L and uplift capacity F_u as a function of the helix diameter D_h and helix to core diameter ratio D_h/D_c is depicted in Figure 6 for a given maximum torque applicable (T_{max} = 5MNm).

At low helix diameter, the limiting criterion is the maximum allowable relative embedment ratio L/D_h. Therefore, the evolution of F_u is identical irrespective of the D_h/D_c ratio and the maximum depth L is equal to $8D_h$ (Figure 6(b)).

The uplift capacity increases together with the helix diameter, increasing bending stress at the helix/core connection. For the largest D_h/D_c ratios, this becomes the limiting constraint, marked by a plateau in Figure 6(a) and a decreasing embedment L in Figure 6(b).

For D_h/D_c equal to 5, and D_h ranging between 0.8 and 1.5, the section capacity (torsion + compression) of the screw pile becomes the limiting factor, as the core section is small. Finally, for the lowest D_h/D_c ratios (1.25, 1.5, 2), namely the largest core diameters D_c, the uplift capacity increases up to a maximum and

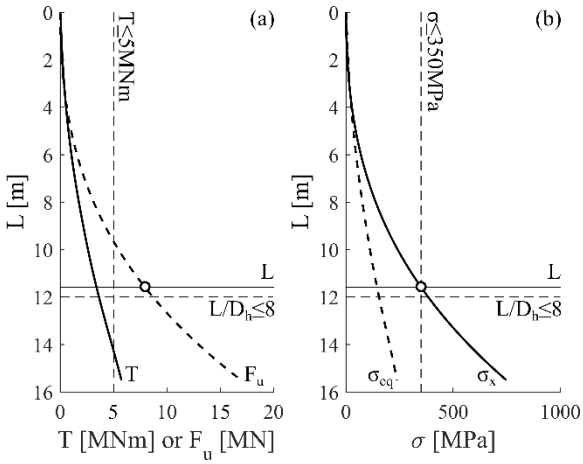

Figure 6 Determination of the maximum embedment and uplift capacity of a screw pile embedded in dense sand for a given geometry (D_h=1.5m, D_h/D_c = 2, t_h = 0.1m, t_c = 0.075m) and maximum installation torque (T_{max} = 5MNm)

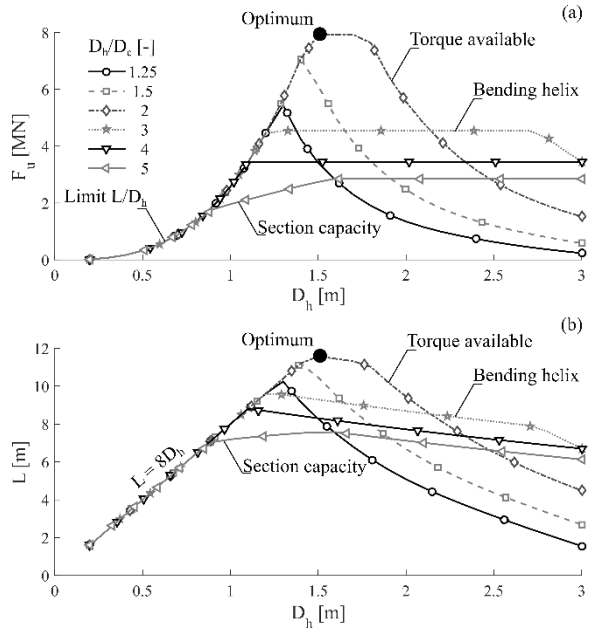

Figure 5 Uplift capacity Fu and installation length L of a screw pile embedded in dense sand as a function of the helix diameter Dh and Dh/Dc ratio, assuming a maximum installation torque equal to 5MNmm

decreases afterwards, because the torque required increases as a function of D_c^3, limiting the maximum embedment depth.

For a maximum torque equal to 5MNm, the optimised geometry is a pile core diameter equal to 1.5m, a D_h/D_c ratio equal to 2 and a length equal to 11.6m. The total uplift capacity is equal to almost 8MN.

3.4 General design optimisation

This analysis was generalised for the three sand densities and maximum torques ranging from 1MNm to 11MNm. For each torque, it is possible to identify the geometry (D_h, L, D_h/D_c) which maximises the screw pile uplift capacity F_u. The results are reported in Figure 7.

The uplift capacity and size of the pile (D_h, L) increase with the maximum torque available, as shown in Figure 7(a,c,d). On the contrary, the optimum helix diameter to core diameter ratio D_h/D_c decreases as the maximum torque

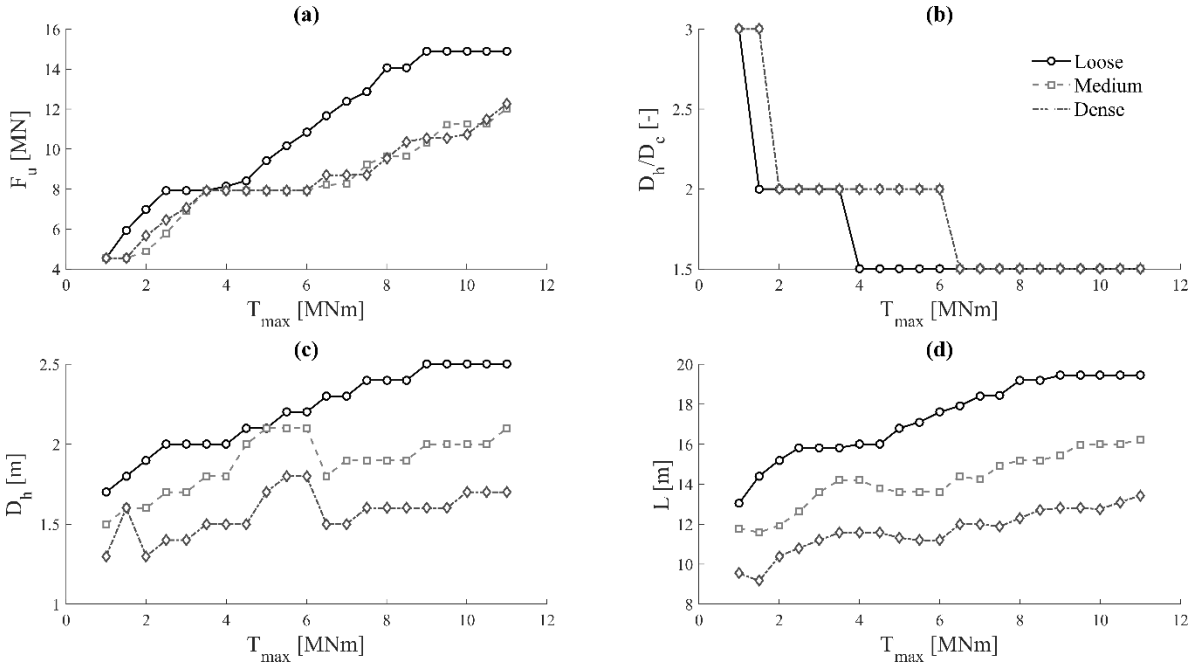

Figure 7 Optimum design for loose (Dr 38%), medium-dense (52%) and dense (82%) HST95 sand as a function of the maximum torque applicable

increases. This is due to the enhanced uplift capacity, generating larger helix bending stress, which is mitigated by increasing the core diameter.

Figure 7(a) compares the maximum uplift capacity available at three different densities as a function of the maximum torque available for installation. Counter-intuitively, the optimised uplift capacity available in loose sand is larger than in medium-dense and dense sands, for a given maximum torque. Indeed, although the soil strength properties are lower for a loose sand, it is possible to embed the screw piles to a greater depth before helix bending becomes critical (Figure 7(d)), with a larger helix diameter (Figure 7(c)) and a lower D_h/D_c ratio (Figure 7(b)).

The order of magnitude of the uplift capacity falls within the range of the requirements for offshore applications (petroleum, wind, wave, aquaculture), providing that adequate installation devices could be developed for offshore applications. Current installation devices able to provide a torque of 3MNm would result in a maximum uplift capacity ranging between 6 and 8 MN.

Finally, some approximations still have to be refined. Indeed, the fabrication capabilities are likely to be a limiting factors (available geometries, welding of the helix). Any decrease in the maximum helix thickness will decrease the uplift capacity. On the contrary, the use of larger steel grade (e.g. f_y =550MPa) will improve it.

4 CONCLUSIONS

A methodology for the design of screw piles in tension has been developed in this paper, based on the combination of several simplified approaches to calculate the screw pile uplift capacity, installation torque and force requirements, and structural constraints (core section or helix bending).

The screw pile uplift capacity is strongly dependent on its embedment, which is mainly limited by the maximum torque available for installation and stress induced by helix bending during uplift.

Results have shown that screw piles are a promising solution for many offshore applications, as the maximum uplift capacity can meet the capacity needs of aquaculture, wave energy converters or floating wind in a wide range of sand densities. However, this would require the development of more powerful installation devices to achieve the targeted maximum torque (and large vertical force).

The methodology could be further improved for more specific cases. The maximum crowd force will be limited by the reaction applicable by the installation device and the possible buckling. The helix will be welded to the core, therefore the maximum stress controlling the helix bending limit may change, especially when cyclic loading is considered. Finally, the maximum displacement required to mobilise the uplift capacity could be limited.

5 ACKNOWLEDGEMENTS

This project has received funding from the European Union's Horizon 2020 research and innovation programme under the Marie Skłodowska-Curie grant agreement No 753156. The authors would also like to acknowledge the support of EPSRC (Grant no. EP/N006054/1: Supergen Wind Hub: Grand Challenges Project: Screw piles for wind energy foundations).

6 REFERENCES

Al-Baghdadi (2018) *Screw piles as offshore foundations : Numerical and physical modelling A dissertation submitted for the degree of Doctor*. University of Dundee.

Al-Defae, Caucis and Knappett (2013) Aftershocks and the whole-life seismic performance of granular slopes, *Géotechnique*, **63**(14), pp. 1230–1244.

Byrne and Houlsby (2015) Helical piles: an innovative foundation design option for offshore wind turbines, *Philosophical Transactions of the Royal Society A: Mathematical, Physical & Engineering Sciences*, **373**(February), pp. 1–11.

Cerfontaine, Davidson, Al-baghdadi, Brown, Knappett *et al.* (2018) Feasibility of screw piles for offshore jacket structures, Part II: numerical modelling, *submitted to Géotechnique*.

Davidson, Al-Baghdadi, Brown, Brennan, Knappett *et al.* (2018a) A modified CPT based installation torque prediction for large screw piles in sand, in Hicks, Pisanò, and Peuchen (eds) *Cone Penetration Testing*. Delft, The Netherlands.

Davidson, Brown, Brennan, Knappett, Augarde *et al.* (2018b) Centrifuge modelling of screw piles for offshore wind energy foundations, in *Proceedings of the 9th Int. Conf. on Physical Modelling in Geotechnics (ICPMG 2018)*. London, UK, pp. 695–700.

Davidson, Brown, Cerfontaine, Al-baghdadi, Knappett *et al.* (2018c) Feasibility of screw piles for offshore jacket structures, Part I: physical modelling, *submitted to Géotechnique*.

Gaudin and O'Loughlin (2018) Geotechnical modelling for offshore renewables, in *Proceedings of the 9th International Conference on Physical Modelling in Geotechnics (ICPMG 2018)*. London, UK, pp. 33–41.

Giampa, Bradshaw and Schneider (2017) Influence of Dilation Angle on Drained Shallow Circular Anchor Uplift Capacity, *International Journal of Geomechanics*, **17**(2), p. 4016056.

Giken (2018) *Silent Piler*. Available at: https://www.giken.com/en/products/silent_piler/ (Accessed: 18 October 2018).

Huang, Tang and Liu (2008) Effects of waves and currents on gravity-type cages in the open sea, *Aquacultural Engineering*, **38**(2), pp. 105–116

Oguz, Clelland, Day, Incecik, López *et al.* (2018) Experimental and numerical analysis of a TLP floating offshore wind turbine, *Ocean Engineering*, **147**(May 2017), pp. 591–605.

Perko (2009) *Helical Piles: A Practical Guide to Design and Installation*. John Wiley & Sons.

Randolph and Gourvenec (2011) *Offshore Geotechnical Engineering*. First Edit. London: CRC Press.

Timoshenko and Woinowky-Krieger (1959) *Theory of Plates and Shells*. Second Edi. McGraw-hill.